No evidence of a human influence on the biodegradation of terrestrial dissolved organic matter (DOM) in Alpine fluvial networks

Thibault Lambert[1,*], Pascal Perolo[1], Nicolas Escoffier[1], Marie-Elodie Perga[1]

[1] Faculty of Geoscience and Environment, Institute of Earth Surface Dynamics, University of Lausanne, Lausanne, Switzerland

[*] corresponding author

Thibault Lambert thibault.lambert@unil.ch

Pascal Perolo pascal.perolo@unil.ch

Nicolas Escoffier nicolas.escoffier@unil.ch

Marie-Elodie Perga marie-elodie.perga@unil.ch

Abstract

The influence of human activities on the role of inland waters in the global carbon (C) cycle is poorly constrained. In this study, we investigated the impact of human land use on the sources and biodegradation of dissolved organic matter (DOM) and its potential impact on bacterial respiration in ten independent catchments of the Lake Geneva Basin. Sites were selected along a gradient of human disturbance (agriculture and urbanization) and were visited twice during the wet season. Bacterial respiration was measured in parallel to DOM bioavailability in dark bioassays, and the influence of human land uses on DOM sources, composition and reactivity was assessed from fluorescence spectroscopy. Bacterial respiration was higher in agro-urban streams but was related to a short-term bioreactive pool (0-6 days of incubation) from autochthonous origin which relative contribution to the total DOM pool increased with the degree of human disturbance. On the other hand, the degradation of a long-term (6-28 days) bioreactive pool from terrestrial origin was independent from the catchment land use and did not contribute substantially to aquatic bacterial respiration. From a greenhouse gas emission perspective, our results suggest that human activities may have a limited impact on the net C exchanges between inland waters and the atmosphere, as most CO_2 fixed by aquatic producers in agro-urban streams is cycled back to the atmosphere after biomineralization. Although seasonal changes in DOM sources must be considered, the implications of our results likely apply more widely as greater proportion of autochthonous-DOM signature is a common feature in human-impacted catchments. Yet, on a global scale, the influence of human activities remains to be determined given the large diversity of effects of agriculture and urbanization on freshwater DOM depending on the local environmental context.

1. Introduction

Continental surface waters receive more terrestrial carbon (C) than they export toward oceans, leading to the conceptualization of inland waters as active pipes that process, emit and store C during its transit from lands to oceans (Cole et al., 2007). Within this framework, the mineralization of terrestrial dissolved organic matter (DOM) by aquatic heterotrophic bacterial communities is a key process by which terrestrial C returns to the atmosphere through CO_2 emissions (Fasching et al., 2014; Lapierre et al., 2013; Mayorga et al., 2005). The study of DOM transport and transformation along fluvial networks is therefore of primary importance, yet a major gap in knowledge revolves around the impact of human activities on the reactivity and bacterial use (i.e., respiration or allocation to biomass) of terrestrial DOM in inland waters (Creed et al., 2015; Xenopoulos et al., 2021).

Agricultural and urban land uses are major catchment features impacting DOM sources and composition in aquatic ecosystems from local (Wilson and Xenopoulos, 2009) to regional scales (Lambert et al., 2017; Williams et al., 2016). Streams draining agricultural landscapes and/or urban catchments are commonly enriched in DOM of low molecular weight compared to streams draining forested catchments whereby DOM is dominated by aromatic, high molecular weight compounds (Lambert et al., 2017; Williams et al., 2010). Greater proportions of lower molecular weight compounds in agro-urban streams can be the consequence of a greater autochthonous algal production and bacterial activity in nutrient-enriched waters (Fuß et al., 2017; Lu et al., 2014; Williams et al., 2010; Wu et al., 2019), reduced hydrological connection with terrestrial sources (Giling et al., 2014; Parr et al., 2015), or transfer of less humified soil organic matter due to agricultural practices (Humbert et al., 2020; Lambert et al., 2017; Landsman-Gerjoi et al., 2020). As lower molecular weight molecules are typically more labile and easily available for uptake to bacterial communities (Berggren et al., 2010; Catalán et al., 2017; Kaplan and Bott, 1989), greater DOM processing can be expected in agro-urban streams (Hosen et al., 2014; Parr et al., 2015). However, the destabilization of a stock of soil organic material built before the conversion of forests or wetlands for agriculture or urban development can lead to the mobilization of large amounts of humic and highly aromatic DOM into surface waters (Ekblad and Bastviken, 2019; Graeber et al., 2012; Hu et al., 2016; Petrone et al., 2011). As a consequence, the impact of human land uses on the dynamic of DOM in inland waters may be highly diverse depending on how agriculture and urbanization affect DOM sources, content, and composition as well as external drivers such as inorganic nutrients known to regulate bacterial DOM processing (Guillemette and del Giorgio, 2012; Reche et al., 1998).

Different scenarios about the consequences on net C exchanges for surface waters can be envisaged depending on the impact of human land uses on freshwater DOM. First, increasing delivery of colored and aromatic terrestrial DOM can lead to increase CO_2

emissions supposing that this terrestrial material gets respired by bacterial communities (Fasching et al., 2014; Lapierre et al., 2013). Second, increase in the export of low molecular weight DOM, either derived from terrestrial sources or produced in-stream, can result in more DOM respired and emitted as CO_2 into the atmosphere (Bodmer et al., 2016; Borges et al., 2018). However, if changes in DOM composition result from an enhancement in aquatic primary production, enhanced respiration of autochthonously-produced DOM shall not lead to higher net CO_2 emissions since the amount of C emitted into the atmosphere would be lower or equivalent to the amount of CO_2 previously fixed by primary aquatic producers. An alternative scenario would be that the release of simple and labile organic compounds derived from autochthonous sources enhances the degradation of terrestrial aromatic DOM by the so-called priming effect (Bianchi, 2011), inducing a final net increase of C emitted to the atmosphere. The priming effect is a process through which labile pool of DOM can enhance ("prime") the degradation of a more recalcitrant DOM pool based on interactions between microbial communities and/or changes in their functions (Guenet et al., 2010; Kuzyakov et al., 2000) but its occurrence in aquatic ecosystems is highly debated (Attermeyer et al., 2014; Bengtsson et al., 2018; Lambert and Perga, 2019). To determine how human activities may impact the mineralization of terrestrial DOM and infer the consequence on the active role of inland waters into the global C cycle, it is therefore necessary to evaluate the consequences on DOM sources, composition, but also DOM bioavailability and to identify which fraction of the DOM pool fuels respiration. This information is critical to establish the role of human land uses on the linkage between terrestrial and aquatic ecosystems.

In this study, we aimed to investigate the impact of human land uses on the role of inland waters as bioreactors with regard to the processing of terrestrial DOM. Water samples were collected twice during the wet season in ten independent catchments selected along a gradient of human pressure (agriculture and urbanization) in the Lake Geneva Basin. Patterns in DOM degradation were investigated based on standardized dark degradation experiments and by the consumption of specific compounds of low molecular weights. Decreases in dissolved organic carbon (DOC) concentrations and changes in DOM composition (assessed by fluorescence spectroscopy) during incubations were used to unravel the contribution of different fractions to the bulk DOM kinetic degradation as well as to the bacterial respiration measured under field conditions. With this approach combining field work and laboratory experiments, we specifically aimed to identify the origin of DOM contributing to bacterial respiration in human-impacted streams and to evaluate the impact of human activities on the biodegradation of terrestrial DOM in Alpine fluvial networks.

2. Material and methods

2.1 Study sites and sampling

Stream and river waters were collected in ten independent tributaries of Lake Geneva, the largest lake of Western Europe located at the border between France and Switzerland in the Western Alps (Figure 1). Lake Geneva lies in the Alpine foreland between the Alps and the Jura mountains and was carved during Quaternary glaciations mostly into the Tertiary Molasse. Drainage areas of streams and rivers ranged from 11 to 5240 km^2, Strahler order from 2 to 7, mean elevation from 614 to 2124 m, and land cover was dominated by forests (39±19%), croplands (30±22%), grasslands (13±14%), and urban areas (11±14%) according to the Swiss Federal Office for the Environment (FOEN). Agriculture is dominated by non-irrigated arable lands and vineyards, and forests by coniferous and broad-leaved trees. Selected streams and rivers drained a mosaic of land cover categories and were classified as agro-urban or forest-grassland streams if the sum of croplands and urban areas extents was higher or lower than 50%, respectively (Table 1).

Samples were collected on two occasions, at the end of autumn between the 13th and 14th of November 2018 and at the end of winter between the 5th and 7th of March 2019. Campaigns were thus carried out during the wet season, i.e., when high discharge conditions may favor greater export of terrestrial DOM (Lambert et al., 2013). The only exception was the Rhône River, that experiences higher water discharge in summer due to the glacio-nival regime of the river (Loizeau and Dominik, 2000). Water temperatures during field campaigns were 10.1±1.8 °C and 6.6±1.1 °C, respectively, but discharge and precipitation conditions at the time of collection were similar (FOEN data). Water was collected below surface in 2 L acid-washed high-density polyethylene (HDPE) bottles and filtered on site. A known volume of water (between 1000 and 1500 mL) was filtered on pre-combusted (450°C for 4 h) Whatman glass fiber filters (GF/F grade, 0.7 µm nominal pore size, 47 mm diameter) for chlorophyll a (Chl*a*) measurements. This filtered water was either stored in 1L acid-washed HDPE bottles for further use in the incubation experiments and the measurements of bacterial metabolism, as described below, or further filtered at 0.2 µm with polyethersulfone (PES) syringe encapsulated filters for dissolved organic carbon (DOC), colored and fluorescent DOM (CDOM and FDOM), soluble reactive phosphorus (SRP), and dissolved inorganic nitrogen (DIN) measurements. Syringe encapsulated filters were first rinsed with ultrapure water (60 mL) in the laboratory and then with 15-20 mL of water from the sampling site before collecting samples. Samples for DOC concentrations were stored in 40 mL acid-washed glass vials with polytetrafluoroethylene (PTFE)-coated septa, and samples for CDOM and FDOM were stored in 40 mL acid-washed amber glass vials with PTFE-coated septa. Samples for SRP, and DIN were stored separately in 50 mL sterile centrifuge tubes. All samples and filters were brought back to the laboratory within 3 hours in cool and dark conditions. Samples for SRP and Chl*a* measurements were frozen at -21°C until analysis. Other samples were stored in a dark chamber at 4-5°C until analysis typically done within the following two weeks.

2.2 Characterization of DOM degradation kinetics

Incubations were prepared once back to the laboratory. Water samples previously filtered on site at 0.7 µm were divided into 250 mL acid-washed glass flasks and incubated for 28 days in the dark at 20°C. Different subsets of flasks (in triplicates) were prepared and sacrificed for DOC measurements and DOM characterization every 3-5 days for the first 10 days and then every 5-8 days up to day 28. Samples were filtered at 0.2 µm with PES syringe encapsulated filters as described above and stored in a dark chamber at 4-5°C. DOC measurements were done within 48h after collection, and CDOM and FDOM analyses over the following week. Dissolved oxygen depletion during the incubations was avoided by leaving a large headspace within the glass flasks and by a regular (every 3-4 days) renewal of the headspace.

Several models can be used to characterize DOM degradation kinetic. Here we applied a first-order exponential decay model in order to derive a decay constant describing the overall dynamic of DOM degradation (Lambert and Perga, 2019; Lu et al., 2013; Shang et al., 2018) as well as the size of the short- and a long-term reactive carbon pools (STRC and LTRC, respectively). Decreasing DOC concentrations during the incubations were modeled using GraphPad Prism 8 software according to the following equation:

$$DOC(t) = DOC_{cons} \times e^{-k*t} + DOC_{residual}$$

where DOC(t) (in mg L^{-1}) is the DOC concentration measured at the incubation time t (in days), DOC_{cons} (in mg L^{-1}) the amount of DOC consumed at the end of the incubation, *k* the decay constant (mg C d^{-1}), and $DOC_{residual}$ (in mg L^{-1}) the concentration of the residual pool remaining in solution at the end of the incubation. Biodegradable DOC (BDOC) was calculated as the difference in DOC between the initial and final time. Furthermore, we used the *k* decay constant from the model to quantify the STRC and LTRC pools: STRC was defined as the amount of DOC consumed within the first six days of incubation and the LTRC as the amount of DOC degraded between days 6 and 28. The separation between STRC and LTRC pools was based on a breakpoint in the degradation curves observed around the 6^{th} day of incubation in almost all experiments. Finally, changes in DOM composition during the incubations were also monitored by fluorescence measurement coupled to parallel factor analysis (PARAFAC) as described below.

2.3 Degradation of low molecular weight compounds

We also determined the consumption of low molecular weight compounds including carbohydrates (CAR), carboxylic and acetic acids (C&AA), and amino acids (AA) using Biolog Ecoplates ® (Garland and Mills, 1991; Weber and Legge, 2009, 2010). Ecoplates ® are 96-well microplates containing 31 different carbon substrates (in triplicates) plus a tetrazolium dye. The bacterial respiration activity associated with a specific substrate reduces the tetrazolium

dye and produces a color measurable at 590 nm in absorbance. The intensity of color development in color can be related to the amount of substrate consumed (e.g., Berggren and del Giorgio 2015). Water from each site (125 µL) filtered at 0.7 µm was added to each well of one Ecoplates ® per site, which was then incubated in the dark at 20°C for 3 to 9 days until the average well color development (AWCD) reached an asymptote. The absorbance at 590 nm was measured with a TECAN microplate reader one to two times per day. Color development of each carbon substrate was calculated as the blank-corrected absorbance at the time when the AWCD was closest to 0.5 (0.51±0.11, n = 60) following recommendations of Weber and Legge (2010). Carbon substrates were then classified as CAR, C&AA, or AA according to Weber and Legge (2009). The color development for each of these categories was calculated as the mean of the color of the respective substrates normalized by the AWCD. While Ecoplates ® also include other organic compounds such as polymers or amines/amides, we focused in this study on the consumption of low molecular weight compounds known to support bacterial respiration (Kaplan and Bott, 1989).

2.4 Bacterial respiration measurements

The 0.7 µm-filtered waters used for incubation experiments were also used to measure bacterial respiration (BR) in stream and river waters, ensuring comparability between water quality and bacterial metabolism. BR was determined from the decrease in dissolved oxygen (DO) in 60 mL borosilicate serum bottles filled with water, sealed with a butyl stopper and crimped with an aluminum cap without headspace (3 serum bottles per site). These vials were equipped with SP-PSt7 oxygen planar sensor spots (PreSens) in order to follow DO consumption after 24h of incubation in the dark at 20°C. Initial (1h after the start of incubation) and final DO was recorded using a PreSens Fibox 4 equipped with a fiber-optic oxygen transmitter. Calibration of the PreSens Fibox 4 (two-point calibration at 0 and 100% oxygen saturation) was performed and verified before measurements. BR data were converted into carbon units using a respiratory quotient of 1.

2.5 Analytical methods

DIN (defined as the sum of nitrate, ammonium and nitrite) was measured by ion chromatography (Metrohm instrument). SRP was determined by spectrophotometry using the ammonium molybdate-potassium antimonyl tartrate method (AFNOR, 2005). DOC concentrations were measured with a total organic carbon analyzer (TOC-L Series, Shimadzu), with a detection limit of 0.01 mg L^{-1} and a precision better than ±5% based on duplicates and standards. Chl*a* concentrations were determined by spectrophotometry after ethanol extraction (90%). Frozen filters were put in 15 mL sterile centrifuge tubes in which 10 mL of ethanol (90%) were added. Tubes were vigorously shaken and then installed in an

ultrasonic bath at 70°C for 10 min. Tubes were then stored in a dark chamber for a night, centrifuged 5 min at 4000 rpm and then 10 min at 4000 rpm. Chl*a* concentrations were determined from absorbance at 665 nm after correction of sample turbidity concomitantly measured at 750 nm. Absorbance for CDOM was measured with a Lambda 365 UV/vis spectrophotometer (Perkin Elmer) from 200 to 700 nm (1 nm increment) using a 10 cm quartz cuvette. Napierian absorption coefficients were calculated according to

$$a_\lambda = 2.303 \times A_\lambda / L,$$

where a_λ is the absorption coefficient (m^{-1}) at wavelength λ, A_λ the absorbance at wavelength λ and L the path length of the optical cell in m. Spectral slopes for the intervals 275–295 and 350–400 nm were determined from the linear regression of the *log*-transformed a spectra versus wavelength and used to determine the slope ratio (S_R). The slope ratio S_R, calculated as the ratio of $S_{275–295}$ to $S_{350–400}$, is inversely related to the molecular weight distribution of DOM (Helms et al., 2008).

FDOM was measured with a Fluorolog-3 spectrofluorometer (Horiba) using a 1 cm quartz cuvette across excitation wavelengths of 270 – 450 nm (5 nm increment) and emission wavelengths of 300 – 500 nm (2 nm increment) in order to build excitation-emission matrices (EEMs). Lamp intensity and instrument calibration were systematically verified before running samples. EEMs were acquired in sample emission to lamp reference mode, and a correction matrix provided by the manufacturer in both excitation and emission dimensions was automatically applied during acquisition. EEMs were then decomposed into individual components using PARAFAC algorithms (Stedmon et al., 2003). Additional samples collected in Lake Geneva and in the Rhône Basin upstream of Lake Geneva were included in the model (total numbers of EEMs > 800). EEMs preprocessing (Raman scattering removal and standardization to Raman units) was performed prior to the PARAFAC modeling. Normalization was done using a Milli-Q water sample run the same day as the sample. An eight components PARAFAC model was obtained using the drEEM 0.3.0 Toolbox (Murphy et al., 2013) for MATLAB (MathWorks, Natick, MA, USA). Split-half analysis, random initialization and visualization of residuals EEMs were used to test and validate the model. The positions of maximums peaks of the PARAFAC components were compared to previous studies with the open fluorescence database OpenFluor using the OpenFluor add-on for the open-source chromatography software OpenChrom (Murphy et al., 2014). The maximum fluorescence F_{Max} values of each component for a particular sample provided by the model were summed to calculate the total fluorescence signal F_{Tot} of the sample in Raman units. The relative abundance of any particular PARAFAC component X was then calculated as $\%C_X = F_{Max}(X)/F_{Tot}$. Precision of EEMs-PARAFAC, based on replicate measurements (n = 5) of different samples, was ±0.001 R.U. for F_{Max} values of components C1 to C5 and ±0.003 R.U for F_{Max} values of components C6 to C8, and ±0.2% for $\%C_X$ for components C1 to C5 and

±0.5% for components C6 to C8. Finally, the variations of PARAFAC components during incubations were expressed as $(F_{Max}(X)_{tf} - F_{Ma}(X)_{t0})/F_{Max}(X)_{t0}$ with t0 and tf the initial and final values of F_{Max}, respectively. Based on the accuracy of EEM-PARAFAC measurements estimated by replicate measurements (see above), we considered variations to be significant if the median of response ratio was higher than ±0.05 for components C1 to C5 and ±0.1 for components C6 to C8.

2.6 Statistical analyses

Differences in water quality, DOM degradability, BR and consumption of low molecular weight compounds between agro-urban and forest-grassland streams were tested with a Mann Whitney unpaired *t*-test at 0.05 confidence interval level. Differences between the sampling periods were investigated by paired *t*-tests. The level of significance was set to 0.05. The ROUT method implemented in the GraphPad Prism 8 software was used to identify potential outliers. A principal component analysis (PCA) was performed to investigate the importance of human land uses on water quality relative to other geomorphological features (e.g. mean elevation) of the study sites. The data selected for the PCA were DOC, SRP, DIN, and the relative abundance of PARAFAC components collected during the two main campaigns. The PCA was done using the *prcomp* function in the R software, and the *factoextra* package was used to identify the variables that contribute the most to the first two dimensions of the PCA. The sum of cropland and urban areas extents were used as descriptive variables in the PCA biplot.

3. Results

3.1 Water quality and DOM composition across catchments

Hydro-climatic conditions were similar for the two sampling campaigns that occurred during high winter base flow level and no significant difference was found in the overall water quality between the two campaigns (not shown). However, significant differences were observed between sampling sites depending on the dominant land cover (Figures 2 and 3). Chl*a* (total range of variation between sites and periods from 0.2 to 54.9 µg L^{-1}), SRP (from 0.7 to 29.3 µg L^{-1}), DIN (from 0.3 to 8.8 mg L^{-1}), and DOC (from 0.7 to 5.9 mg L^{-1}) concentrations were higher in agro-urban streams that were also characterized by DOM of lower molecular weight (higher S_R values) and higher BR values (Figure 2).

Eight PARAFAC components were identified in our study sites (Table 2, Supplementary Figure S1), all of which having been already described in previous studies (Graeber et al., 2012; Lambert et al., 2017; Massicotte and Frenette, 2011; Stedmon et al., 2011; Stedmon and Markager, 2005; Williams et al., 2016; Yamashita et al., 2010). Components included three humic-like fluorophores (C1, C3, C4), one fulvic-like fluorophore (C2), two microbial protein-

like fluorophores (C5 and C6), and the common tryptophane (C7) and tyrosine (C8) protein-like fluorophores. All components exhibited higher F_{Max} values in agro-urban streams, although the most notable increases were observed for protein-like fluorophores (Figure 3).

The two first components of the PCA explained 72.4% of the variance (Figure 4). The first principal component (PC1) was related to protein-like components C6 to C8, DOC and SRP (positive scores) and to humic-like components C2 to C4 (negative scores), whereas the second principal component (PC2) was related to higher C5, DOC and DIN concentrations (positive scores) and lower C1 (negative score). The results of the PCA showed that the variability in DOM composition and nutrient loadings was largely driven by land uses (Figure 4). Scores along PC1 were positively related to croplands (Pearson r = 0.49, p = 0.0265), urban areas (Pearson r = 0.63, p = 0.0027) and negatively to forest (Pearson r = -0.72, p = 0.0003) and grasslands (Pearson r = -0.48, p = 0.0295), but not to catchment area (Pearson r = -0.04, p = 0.86), Strahler order (Pearson r = 0.13, p = 0.57) or mean elevation (Pearson r = -0.32, p = 0.18). No relationship was found between PC2 and geomorphological properties of sampling sites, suggesting an in-stream origin for the components C1 and C5. Based on the optical properties of PARAFAC components (Table 2), PC1 represented a shift in the dominant composition of DOM from terrestrial (components C2-C4) to autochthonous (C6-C8) signatures as human disturbance (croplands + urban areas) increases. PC2, however, reflected the in-stream generation of DOM through photodegradation (C1) and bacterial processing of DOM (C5).

3.2 Kinetics of bacterial DOM degradation and consumption of low molecular weight compounds

All incubations were successfully modeled by a first order exponential decay model (r^2 = 0.98±0.02), and we estimated the decay constants and the amounts of BDOC, STRC and LTRC pools for all experiments (Figure 5). BDOC ranged from 0.2 to 2.3 mg L^{-1} (mean = 1.0±0.6 mg L^{-1}), corresponding to 9.7 to 57.6% of initial DOC (mean = 33.8±11%). Higher amount of BDOC in agro-urban streams was accompanied by higher decay constants (from 0.01 to 0.26 d^{-1}, mean = 0.12±0.07 d^{-1}) and greater availability of STRC (from 0.01 to 1.3 mg L^{-1}, mean = 0.5±0.4 mg L^{-1}) but no significant difference was observed regarding the amount of LTRC (from 0.1 to 1.0 mg L^{-1}, mean = 0.5±0.3 mg L^{-1}) across stream categories. Both the STRC and LTRC pools were positively correlated with DOC concentrations (Pearson r = 0.79, p < 0.0001 and Pearson r = 0.68, p = 0.0013, respectively), leading to a positive but weak relationship between the STRC and LTRC pools (Person r = 0.49, p = 0.03). STRC was correlated to all components when expressed in FMax values, but only with protein-like components when expressed as a relative contribution to the total fluorescence signal, suggesting an autochthonous origin for this reactive C. On the contrary, the LTRC related to

FMax values of C1-C4 components but not with the protein-like components, implying that this reactive C originated from terrestrial inputs. The total amount of BDOC, decay constants and the size of STRC were significantly related to the C6-C8 protein-like components (Figure 6). There was however no relationship between the decay constant k and LTRC.

The S_R values decreased in all experiments (Supplementary Figure S2), indicating an increase in the average molecular weight of DOM during incubations as low molecular weight compounds were preferentially degraded. Regarding the evolution of the different fractions of DOM during incubations, no significant changes in F_{Max} values were observed for humic-like components during incubations (Figure 7). Component C5, however, tended to be produced upon bacterial activity. On the contrary, the other protein-like components C6 – C8 were consumed during incubations. Finally, the consumption of low molecular weights compounds was greater in agro-urban streams for AA and CAR molecules, but no difference was observed regarding the degradation of C&AA (Figure 8).

4. Discussion

The spatial variability in water quality and DOM sources and composition observed in streams and rivers of the Lake Geneva basin during the wet season echoes numerous previous works illustrating the impact of human activities on freshwater ecosystems (Lambert et al., 2017; Shang et al., 2018; Wilson and Xenopoulos, 2009). Our study further reveals that the enrichment in protein-like, low molecular weight DOM in agro-urban streams increased the total amount of bioavailable DOM as well as bacterial respiration. However, we found no evidence of an impact of human activities on the degradation of terrestrial DOM, nor that the latter contributed to ecosystem respiration.

4.1 Origin and biodegradability of DOM in agro-urban streams

DOC concentrations in agro-urban streams of the Lake Geneva Basin were higher compared to those measured in forest-grassland streams (Figure 2) and these increases were accompanied by a shift in DOM composition toward more autochthonous signatures (Figure 4). Effects of agriculture and urbanization on freshwater DOM can vary widely depending on the environmental context and catchment properties (Shang et al., 2018; Stanley et al., 2012), and in our study we attributed this pattern to the combination of enhanced autochthonous production and higher transfer of terrestrial material. Enrichment in nutrients and increased light exposure in agriculture and urban streams can promote primary production (Catford et al., 2007; Stanley et al., 2012; Taylor et al., 2004), and greater algal biomass in our study sites was evidenced by higher Chl*a* concentrations (Figure 2) and the subsequent release of protein-like components (C6 – C8) related to algal DOM (Figure 3, Table 2). Although C5 also relates to autochthonous biological production (Stedmon et al., 2011), its accumulation during

incubation experiments implies that this component reflected DOM recently produced by bacterial activity (Figure 7). Higher F_{Max} values of C5 in human-impacted catchments thus represented a positive feedback loop where greater primary production enhanced bacterial activity that shaped DOM composition toward a more bacterial signature (Harfmann et al., 2019; Williams et al., 2010). Although of lower amplitude, higher F_{Max} values of components associated with terrestrial inputs (C2 – C4, Table 2) and/or photobleaching (C1) indicated a more efficient export of terrestrial material in agro-urban streams. As urbanization tends to limit the hydrological connection between terrestrial and aquatic ecosystems (e.g. Hosen et al. 2014), it is likely that this pattern reflected greater erosion of agricultural soils (Celik, 2005; Graeber et al., 2012). While it was not the purpose of this study to investigate more deeply the links between human land uses and DOM sources, our results suggest that agriculture and urbanization can act in concert to disturb both terrestrial and aquatic sources of DOM leading to greater amounts of both humic- and protein-like components in agro-urban streams compared to more natural land cover.

Along with changes in DOM sources and composition, the bacterial consumption of DOM was strongly impacted by croplands and urbanization (Figure 5). The positive effect of human land use on the total amount and decay constants of bioavailable DOM agrees with previous studies (Hosen et al., 2014; Parr et al., 2015), but our results further link this effect to the generation of a highly reactive pool of organic molecules derived from in stream primary production. Algae are known to be a major source of low molecular weight compounds in aquatic ecosystems through exudation and cell lysis (Kaplan and Bott, 1989) which are rapidly taken up by heterotrophic bacteria (Descy, 2002). A higher consumption of amino acids and carbohydrates concomitant with higher Chl*a* concentrations in agro-urban streams agrees with the generation of labile molecules derived from primary production. The loss of protein-like components paralleled by a shift in the molecular weight to during incubations also evidences the efficient degradation of this DOM from algal origin. Moreover, the strong relationships between the amount of BDOC, the decay constants *k*, and the size of the STRC pool with the initial contribution of protein-like components C6-C8 (Figure 6) provide another evidence that greater DOM bioavailability in agro-urban streams resulted from greater in-stream production.

4.2 Biodegradability of terrestrial DOM is not related to land use

Contrary to STRC, we found no evidence that human land uses impact the loss of terrestrial DOM upon bacterial degradation. The LTRC pools were indeed similar across agro-urban and forest-grassland streams despite a higher content in inorganic nutrients, a greater bacterial activity, and a greater share of freshly produced autochthonous DOM in agro-urban streams. In line with a recent study carried out in Swedish inland waters (Soares et al., 2019), the STRC and LTRC pools were comparable in size but no evidence of interaction was

observed between the bioavailability of DOM on short and long timescales. The positive but weak relationship between STRC and LTRC likely reflected a greater amount of bioavailable DOM as human disturbance increased, as the latter enhanced both primary production and terrestrial export. Moreover, each pool related to specific DOM fractions. Similar observations were reported in Swedish rivers (Soares et al., 2019), in southern Québec (Guillemette and del Giorgio, 2011), or also in the Hudson River (del Giorgio and Pace, 2008). Overall, our findings are in good agreement with the idea that STRC is sustained by algal growth, whereas the consumption of DOC at longer timescales is rather related to terrestrial inputs of DOM (references above).

Although a substantial amount of terrestrial DOM was consumed by heterotrophic bacteria, the terrestrial (C2-C4) and photoproduced (C1) components showed no significant variations during incubations (Figure 7) despite the ability of bacterial communities to degrade complex aromatic molecules (Catalán et al., 2017; Fasching et al., 2014; Logue et al., 2016). While the stability of the C1 component during bioassays is consistent with the fact that photoproduced molecules may be resistant to further bacterial degradation (Tranvik et al., 2001), the lack of variation of C2-C4 components may reflect an equilibrium between the bacterial consumption and production of molecules contributing to the humic-like signatures. Experimental and field studies have shown that heterotrophic bacterial communities are able to produce molecules fluorescing in the region of EEMs commonly attributed to humic-like material from terrestrial origin (Amaral et al., 2016; Fox et al., 2017; Guillemette and del Giorgio, 2012). It is therefore possible that the alteration in the composition of terrestrial DOM upon bacterial activity may not have been captured by optical measurements. Addressing this point would require the characterization of DOM at the molecular level (e.g., Kim et al., 2006).

4.3 Linking bacterial respiration to DOM origin and implication of human activities on the role of inland water in the C cycle

The loss of terrestrial DOM through bacterial mineralization as it moves along fluvial networks contributes to CO_2 emissions toward the atmosphere (Lapierre et al., 2013), and human activities are expected to impact the role of inland waters in the global carbon cycle by disturbing DOM sources and composition (Xenopoulos et al., 2021). Our results indeed confirmed that human land use impacted DOM sources, composition and biodegradability. However, they also evidenced that during the wet season and at the scale of small catchments, such modifications may only have a null or minor effect on C budget and atmospheric exchanges. Higher BR in agro-urban streams was indeed mostly related to the accumulation and mineralization of molecules generated in-stream by aquatic primary producers (Figure 9A), although the photodegradation of terrestrial DOM could also have contributed to increase BR through the transformation of complex and aromatic molecules into compounds of lower

molecular weight (Bertilsson and Tranvik, 1998) as suggested by the positive relationship between BR and C1 (Figure 9B). From a CO_2 emission perspective, this implies that most of the C released toward the atmosphere upon bacterial respiration corresponded to atmospheric CO_2 previously fixed by aquatic producers and converted into biomass.

Finally, despite the large range of size of our sampling sites (Table 1), we found no relationship between Strahler order (ranging from 2 to 7) and DOM composition and reactivity. This observation contrasts with a recent study where stream order (ranging from 1 to 4) correlated negatively with humic-like DOM but positively with protein-like DOM (Shang et al., 2018), a pattern consistent with a general conceptual trend describing DOM transformations along the fluvial continuum. Indeed, the control of DOM dynamic along the river continuum is expected to shift from a dominant influence of terrestrial inputs in the headwaters to a dominant influence of in-stream removal and autochthonous production as stream order increases (Creed et al. 2015). In our study, however, human land uses had a major role in controlling DOM sources and reactivity at the basin scale (Figure 4). The only exception was a positive correlation between Strahler order and the relative proportion of C5 (Supplementary Figure S3), indicating that the degradation of autochthonous DOM in agro-urban streams led to a bacterial imprint on the DOM pool that persists along the aquatic continuum (Harfmann et al., 2019; Williams et al., 2010).

5. Conclusion

In this study, human land uses were found to alter the terrestrial and aquatic sources of freshwater DOM. Greater autochthonous production of DOM in agro-urban streams led to higher amounts of bioavailable DOM, stimulating ecosystem respiration while no influence on the loss of terrestrial DOM was observed. Despite a dominant influence on DOM composition and reactivity at the basin scale, we found that human land uses had a limited effect in terms of net C flux exchanges between inland waters and atmosphere related to DOM mineralization by heterotrophic bacterial communities.

Although our study focused mainly on small catchments during the wet period, our results are likely not limited to the Lake Geneva Basin considering that an enrichment in protein-like DOM due to greater autochthonous production is a recurrent observation in agricultural and urban catchments (Stanley et al., 2012; Xenopoulos et al., 2021). However, caution should be taken when extrapolating the impact of human activities on the role of inland waters on the C cycle. Indeed, the net effects of agriculture and urbanization on freshwater DOM vary widely depending on the environmental context (Stanley et al., 2012), leading to apparent opposite effects on BDOC. Thus, while our results are in line with previous works (Hosen et al., 2014; Parr et al., 2015), they contrast with studies reporting no influence of

human land uses on the bacterial consumption of DOM (Kadjeski et al., 2020; Lu et al., 2013) or higher DOM degradability in agricultural streams (Shang et al., 2018). Therefore, additional works on the links between human activities and DOM reactivity and fate are needed in order to fully assess the future of inland waters in the context of the global C cycle.

Author Contributions: T. L. conceived the study with contribution from M.-E. P. T. L., P. P., and N. E. collected field samples. T. L. made laboratory analysis. T.L. drafted the manuscript which was substantially commented upon and amended by M.-E. P., P. P., and N. E. All co-authors approved the manuscript.

Competing interests: The authors declare that they have no conflict of interest.

Acknowledgements: We thank Laetitia Monbaron and Micaela Faria for assistance in the laboratory and Janine Rüegg for her comments on an initial version of the manuscript. We gratefully acknowledge the anonymous reviewers who provided very constructive and insightful comments on the earlier version of this manuscript.

Financial Support: This study was supported by funding from CARBOGEN FNS 200021_175530

References

AFNOR: NF EN ISO 6878 : Qualité de l'eau Dosage du phosphore - Méthode spectrométrique au molybdate d'ammonium, AFNOR, 2005.

Amaral, V., Graeber, D., Calliari, D. and Alonso, C.: Strong linkages between DOM optical properties and main clades of aquatic bacteria, Limnol. Oceanogr., 61(3), 906–918, doi:10.1002/lno.10258, 2016.

Attermeyer, K., Hornick, T., Kayler, Z. E., Bahr, A., Zwirnmann, E., Grossart, H. P. and Premke, K.: Enhanced bacterial decomposition with increasing addition of autochthonous to allochthonous carbon without any effect on bacterial community composition, Biogeosciences, 11(6), 1479–1489, doi:10.5194/bg-11-1479-2014, 2014.

Battin, T. J., Kaplan, L. A., Findlay, S., Hopkinson, C. S., Marti, E., Packman, A. I., Newbold, J. D. and Sabater, F.: Biophysical controls on organic carbon fluxes in fluvial networks, Nat. Geosci., 1, 95–100, doi:10.1038/ngeo101, 2008.

Bengtsson, M. M., Attermeyer, K. and Catalán, N.: Interactive effects on organic matter processing from soils to the ocean: are priming effects relevant in aquatic ecosystems?, Hydrobiologia, 822(1), doi:10.1007/s10750-018-3672-2, 2018.

Berggren, M. and del Giorgio, P. A.: Distinct patterns of microbial metabolism associated to riverine dissolved organic carbon of different source and quality, J. Geophys. Res. G Biogeosciences, 120, 989–999, doi:10.1002/2015JG002963, 2015.

Berggren, M., Laudon, H., Haei, M., Ström, L. and Jansson, M.: Efficient aquatic bacterial metabolism of dissolved low-molecular-weight compounds from terrestrial sources, ISME J., 4(3), 408–416, doi:10.1038/ismej.2009.120, 2010.

Bertilsson, S. and Tranvik, L. J.: Photochemically produced carboxylic acids as substrates for freshwater bacterioplankton, Limnol. Oceanogr., 43(5), 885–895,

506 doi:10.4319/lo.1998.43.5.0885, 1998.

507 Bianchi, T. S.: The role of terrestrially derived organic carbon in the coastal ocean: A
508 changing paradigm and the priming effect, Proc. Natl. Acad. Sci., 108(49), 19473–19481,
509 doi:10.1073/pnas.1017982108, 2011.

510 Bodmer, P., Heinz, M., Pusch, M., Singer, G. and Premke, K.: Carbon dynamics and their
511 link to dissolved organic matter quality across contrasting stream ecosystems, Sci. Total
512 Environ., 553, 574–586, doi:10.1016/j.scitotenv.2016.02.095, 2016.

513 Borges, A. V., Darchambeau, F., Lambert, T., Bouillon, S., Morana, C., Brouyère, S.,
514 Hakoun, V., Jurado, A., Tseng, H. C., Descy, J. P. and Roland, F. A. E.: Effects of
515 agricultural land use on fluvial carbon dioxide, methane and nitrous oxide concentrations in a
516 large European river, the Meuse (Belgium), Sci. Total Environ., 610–611(August 2017), 342–
517 355, doi:10.1016/j.scitotenv.2017.08.047, 2018.

518 Catalán, N., Casas-Ruiz, J. P., von Schiller, D., Proia, L., Obrador, B., Zwirnmann, E. and
519 Marcé, R.: Biodegradation kinetics of dissolved organic matter chromatographic fractions, a
520 case study in an intermittent river, J. Geophys. Res. Biogeosciences, 122, 131–144,
521 doi:10.1002/2016JG003512, 2017.

522 Catford, J. A., Walsh, C. J. and Beardall, J.: Catchment urbanization increases benthic
523 microalgal biomass in streams under controlled light conditions, Aquat. Sci., 69(4), 511–522,
524 doi:10.1007/s00027-007-0907-0, 2007.

525 Celik, I.: Land-use effects on organic matter and physical properties of soil in a southern
526 Mediterranean highland of Turkey, Soil Tillage Res., 83(2), 270–277,
527 doi:10.1016/j.still.2004.08.001, 2005.

528 Cole, J. J., Prairie, Y. T., Caraco, N. F., McDowell, W. H., Tranvik, L. J., Striegl, R. G.,
529 Duarte, C. M., Kortelainen, P., Downing, J. A., Middelburg, J. J. and Melack, J.: Plumbing the
530 global carbon cycle: Integrating inland waters into the terrestrial carbon budget, Ecosystems,
531 10(1), 171–184, doi:10.1007/s10021-006-9013-8, 2007.

532 Creed, I. F., McKnight, D. M., Pellerin, B. A., Green, M. B., Bergamaschi, B. A., Aiken, G. R.,
533 Burns, D. A., Findlay, S. E. G., Shanley, J. B., Striegl, R. G., Aulenbach, B. T., Clow, D. W.,
534 Laudon, H., McGlynn, B. L., McGuire, K. J., Smith, R. A. and Stackpoole, S. M.: The river as
535 a chemostat: fresh perspectives on dissolved organic matter flowing down the river
536 continuum, Can. J. Fish. Aquat. Sci., 72(8), 1272–1285, doi:10.1139/cjfas-2014-0400, 2015.

537 Descy, J.-P.: Phytoplankton production, exudation and bacterial reassimilation in the River
538 Meuse (Belgium), J. Plankton Res., 24(3), 161–166, doi:10.1093/plankt/24.3.161, 2002.

539 Ekblad, A. and Bastviken, D.: Deforestation releases old carbon, Nat. Geosci., 12(July),
540 doi:10.1038/s41561-019-0394-7, 2019.

541 Fasching, C., Behounek, B., Singer, G. A. and Battin, T. J.: Microbial degradation of
542 terrigenous dissolved organic matter and potential consequences for carbon cycling in
543 brown-water streams, Sci. Rep., 4, 1–7, doi:10.1038/srep04981, 2014.

544 Fox, B. G., Thorn, R. M. S., Anesio, A. M. and Reynolds, D. M.: The in situ bacterial
545 production of fluorescent organic matter; an investigation at a species level, Water Res., 125,
546 350–359, doi:10.1016/j.watres.2017.08.040, 2017.

547 Fuß, T., Behounek, B., Ulseth, A. J. and Singer, G. A.: Land use controls stream ecosystem
548 metabolism by shifting dissolved organic matter and nutrient regimes, Freshw. Biol., 62(3),
549 582–599, doi:10.1111/fwb.12887, 2017.

550 Garland, J. L. and Mills, A. L.: Classification and characterization of heterotrophic microbial
551 communities on the basis of patterns of community-level sole-carbon-source utilization, Appl.
552 Environ. Microbiol., 57(8), 2351–2359, doi:10.1128/aem.57.8.2351-2359.1991, 1991.

553 Giling, D. P., Grace, M. R., Thomson, J. R., Mac Nally, R. and Thompson, R. M.: Effect of

554 Native Vegetation Loss on Stream Ecosystem Processes: Dissolved Organic Matter
555 Composition and Export in Agricultural Landscapes, Ecosystems, 17(1), 82–95,
556 doi:10.1007/s10021-013-9708-6, 2014.

557 del Giorgio, P. A. and Pace, M. L.: Relative independence of dissolved organic carbon
558 transport and processing in a large temperate river: The Hudson River as both pipe and
559 reactor, Limnol. Oceanogr., 53(1), 185–197, doi:10.4319/lo.2008.53.1.0185, 2008.

560 Graeber, D., Gelbrecht, J., Pusch, M. T., Anlanger, C. and von Schiller, D.: Agriculture has
561 changed the amount and composition of dissolved organic matter in Central European
562 headwater streams, Sci. Total Environ., 438, 435–446, doi:10.1016/j.scitotenv.2012.08.087,
563 2012.

564 Guenet, B., Danger, M., Abbadie, L. and Lacroix, G.: Priming effect: bridging the gap
565 between terrestrial and aquatic ecology, Ecology, 91(10), 2850–2861, doi:10.1890/09-
566 1968.1, 2010.

567 Guillemette, F. and del Giorgio, P. A.: Reconstructing the various facets of dissolved organic
568 carbon bioavailability in freshwater ecosystems, Limnol. Oceanogr., 56(2), 734–748,
569 doi:10.4319/lo.2011.56.2.0734, 2011.

570 Guillemette, F. and del Giorgio, P. A.: Simultaneous consumption and production of
571 fluorescent dissolved organic matter by lake bacterioplankton, Environ. Microbiol., 14(6),
572 1432–1443, doi:10.1111/j.1462-2920.2012.02728.x, 2012.

573 Guillemette, F., Leigh Mccallister, S. and Del Giorgio, P. A.: Selective consumption and
574 metabolic allocation of terrestrial and algal carbon determine allochthony in lake bacteria,
575 ISME J., 10(6), 1373–1382, doi:10.1038/ismej.2015.215, 2016.

576 Harfmann, J. L., Guillemette, F., Kaiser, K., Spencer, R. G. M., Chuang, C. Y. and Hernes, P.
577 J.: Convergence of Terrestrial Dissolved Organic Matter Composition and the Role of
578 Microbial Buffering in Aquatic Ecosystems, J. Geophys. Res. Biogeosciences, 124(10),
579 3125–3142, doi:10.1029/2018JG004997, 2019.

580 Helms, J. R., Stubbins, A., Ritchie, J. D., Minor, E. C., Kieber, D. J. and Mopper, K.:
581 Absorption Spectral Slopes and Slope Rations As Indicators of Molecular Weight,Source,and
582 Photoleaching of Chromophoric Dissolved Organic Matter, , 53(3), 955–969, 2008.

583 Hosen, J. D., McDonough, O. T., Febria, C. M. and Palmer, M. A.: Dissolved organic matter
584 quality and bioavailability changes across an urbanization gradient in headwater streams,
585 Environ. Sci. Technol., 48(14), 7817–7824, doi:10.1021/es501422z, 2014.

586 Hu, Y., Lu, Y. H., Edmonds, J. W., Liu, C., Wang, S., Das, O., Liu, J. and Zheng, C.:
587 Hydrological and land use control of watershed exports of dissolved organic matter in a large
588 arid river basin in northwestern China, J. Geophys. Res. Biogeosciences, 121(2), 466–478,
589 doi:10.1002/2015JG003082, 2016.

590 Humbert, G., Parr, T. B., Jeanneau, L., Dupas, R., Petitjean, P., Akkal-Corfini, N., Viaud, V.,
591 Pierson-Wickmann, A. C., Denis, M., Inamdar, S., Gruau, G., Durand, P. and Jaffrézic, A.:
592 Agricultural Practices and Hydrologic Conditions Shape the Temporal Pattern of Soil and
593 Stream Water Dissolved Organic Matter, Ecosystems, 23(7), 1325–1343,
594 doi:10.1007/s10021-019-00471-w, 2020.

595 Kadjeski, M., Fasching, C. and Xenopoulos, M. A.: Synchronous Biodegradability and
596 Production of Dissolved Organic Matter in Two Streams of Varying Land Use, Front.
597 Microbiol., 11(November), 1–14, doi:10.3389/fmicb.2020.568629, 2020.

598 Kaplan, L. A. and Bott, T. L.: Diel fluctuations in bacterial activity on streambed substrata
599 during vernal algal blooms: Effects of temperature, water chemistry, and habitat, Limnol.
600 Oceanogr., 34(4), 718–733, doi:10.4319/lo.1989.34.4.0718, 1989.

601 Kim, S., Kaplan, L. A. and Hatcher, P. G.: Biodegradable dissolved organic matter in a

602 temperate and a tropical stream determined from ultra – high resolution mass spectrometry, ,
603 51(2), 1054–1063, 2006.

604 Kuzyakov, Y., Friedel, J. K. and Stahr, K.: Review of mechanisms and quantification of
605 priming effects, Soil Biol. Biochem., 32(11–12), 1485–1498, doi:10.1016/S0038-
606 0717(00)00084-5, 2000.

607 Lambert, T. and Perga, M.-E.: Non-conservative patterns of dissolved organic matter
608 degradation when and where lake water mixes, Aquat. Sci., 81(4), 64, doi:10.1007/s00027-
609 019-0662-z, 2019.

610 Lambert, T., Pierson-Wickmann, A. C., Gruau, G., Jaffrezic, A., Petitjean, P., Thibault, J. N.
611 and Jeanneau, L.: Hydrologically driven seasonal changes in the sources and production
612 mechanisms of dissolved organic carbon in a small lowland catchment, Water Resour. Res.,
613 49(9), 5792–5803, doi:10.1002/wrcr.20466, 2013.

614 Lambert, T., Bouillon, S., Darchambeau, F., Morana, C., Roland, F. A. E., Descy, J. P. and
615 Borges, A. V.: Effects of human land use on the terrestrial and aquatic sources of fluvial
616 organic matter in a temperate river basin (The Meuse River, Belgium), Biogeochemistry,
617 136(2), 191–211, doi:10.1007/s10533-017-0387-9, 2017.

618 Landsman-Gerjoi, M., Perdrial, J. N., Lancellotti, B., Seybold, E., Schroth, A. W., Adair, C.
619 and Wymore, A.: Measuring the influence of environmental conditions on dissolved organic
620 matter biodegradability and optical properties: a combined field and laboratory study,
621 Biogeochemistry, 149(1), 37–52, doi:10.1007/s10533-020-00664-9, 2020.

622 Lapierre, J. F., Guillemette, F., Berggren, M. and Del Giorgio, P. A.: Increases in terrestrially
623 derived carbon stimulate organic carbon processing and CO 2 emissions in boreal aquatic
624 ecosystems, Nat. Commun., 4, doi:10.1038/ncomms3972, 2013.

625 Logue, J. B., Stedmon, C. A., Kellerman, A. M., Nielsen, N. J., Andersson, A. F., Laudon, H.,
626 Lindström, E. S. and Kritzberg, E. S.: Experimental insights into the importance of aquatic
627 bacterial community composition to the degradation of dissolved organic matter, ISME J.,
628 10(3), 533–545, doi:10.1038/ismej.2015.131, 2016.

629 Loizeau, J. L. and Dominik, J.: Evolution of the upper Rhone river discharge and suspended
630 sediment load during the last 80 years, Aquat. Sci., 62, 54–67, doi:10.1007/s000270050075,
631 2000.

632 Lu, Y., Bauer, J. E., Canuel, E. A., Yamashita, Y., Chambers, R. M. and Jaffé, R.:
633 Photochemical and microbial alteration of dissolved organic matter in temperate headwater
634 streams associated with different land use, J. Geophys. Res. Biogeosciences, 118(2), 566–
635 580, doi:10.1002/jgrg.20048, 2013.

636 Lu, Y. H., Bauer, J. E., Canuel, E. A., Chambers, R. M., Yamashita, Y., Jaffé, R. and Barrett,
637 A.: Effects of land use on sources and ages of inorganic and organic carbon in temperate
638 headwater streams, Biogeochemistry, 119(1–3), 275–292, doi:10.1007/s10533-014-9965-2,
639 2014.

640 Massicotte, P. and Frenette, J. J.: Spatial connectivity in a large river system: Resolving the
641 sources and fate of dissolved organic matter, Ecol. Appl., 21(7), 2600–2617, doi:10.1890/10-
642 1475.1, 2011.

643 Mayorga, E., Aufdenkampe, A. K., Masiello, C. A., Krusche, A. V., Hedges, J. I., Quay, P. D.,
644 Richey, J. E. and Brown, T. A.: Young organic matter as a source of carbon dioxide
645 outgassing from Amazonian rivers, Nature, 436(7050), 538–541, doi:10.1038/nature03880,
646 2005.

647 Murphy, K. R., Stedmon, C. A., Graeber, D. and Bro, R.: Fluorescence spectroscopy and
648 multi-way techniques. PARAFAC, Anal. Methods, 5(23), 6557, doi:10.1039/c3ay41160e,
649 2013.

650 Murphy, K. R., Stedmon, C. A., Wenig, P. and Bro, R.: OpenFluor– an online spectral library
651 of auto-fluorescence by organic compounds in the environment, Anal. Methods, 6(3), 658–
652 661, doi:10.1039/C3AY41935E, 2014.

653 Parr, T. B., Cronan, C. S., Ohno, T., Findlay, S. E. G., Smith, S. M. C. and Simon, K. S.:
654 Urbanization changes the composition and bioavailability of dissolved organic matter in
655 headwater streams, Limnol. Oceanogr., 60(3), 885–900, doi:10.1002/lno.10060, 2015.

656 Petrone, K. C., Fellman, J. B., Hood, E., Donn, M. J. and Grierson, P. F.: The origin and
657 function of dissolved organic matter in agro-urban coastal streams, J. Geophys. Res.
658 Biogeosciences, 116(1), doi:10.1029/2010JG001537, 2011.

659 Reche, I., Pace, M. L. and Cole, J. J.: Interactions of photobleaching and inorganic nutrients
660 in determining bacterial growth on colored dissolved organic carbon, Microb. Ecol., 36(3),
661 270–280, doi:10.1007/s002489900114, 1998.

662 Shang, P., Lu, Y. H., Du, Y. X., Jaffé, R., Findlay, R. H. and Wynn, A.: Climatic and
663 watershed controls of dissolved organic matter variation in streams across a gradient of
664 agricultural land use, Sci. Total Environ., 612, 1442–1453,
665 doi:10.1016/j.scitotenv.2017.08.322, 2018.

666 Soares, A. R. A., Lapierre, J., Selvam, B. P., Lindström, G. and Berggren, M.: Controls on
667 dissolved organic carbon bioreactivity in river systems, , 9(14897), 1–9, doi:10.1038/s41598-
668 019-50552-y, 2019.

669 Stanley, E. H., Powers, S. M., Lottig, N. R., Buffam, I. and Crawford, J. T.: Contemporary
670 changes in dissolved organic carbon (DOC) in human-dominated rivers: Is there a role for
671 DOC management?, Freshw. Biol., 57(SUPPL. 1), 26–42, doi:10.1111/j.1365-
672 2427.2011.02613.x, 2012.

673 Stedmon, C. A. and Markager, S.: Resolving the variability in dissolved organic matter
674 florescence in a temperate estuary and its catchment using PARAFAC analysis., Limnol.
675 Oceanogr., 50(2), 686–697, doi:10.4319/lo.2005.50.2.0686, 2005.

676 Stedmon, C. A., Markager, S. and Bro, R.: Tracing dissolved organic matter in aquatic
677 environments using a new approach to fluorescence spectroscopy, Mar. Chem., 82(3–4),
678 239–254, doi:10.1016/S0304-4203(03)00072-0, 2003.

679 Stedmon, C. A., Thomas, D. N., Papadimitriou, S., Granskog, M. A. and Dieckmann, G. S.:
680 Using fluorescence to characterize dissolved organic matter in Antarctic sea ice brines, J.
681 Geophys. Res. Biogeosciences, 116(3), 1–9, doi:10.1029/2011JG001716, 2011.

682 Taylor, S. L., Roberts, S. C., Walsh, C. J. and Hatt, B. E.: Catchment urbanisation and
683 increased benthic algal biomass in streams: Linking mechanisms to management, Freshw.
684 Biol., 49(6), 835–851, doi:10.1111/j.1365-2427.2004.01225.x, 2004.

685 Tranvik, L., Bertilsson, S. and Letters, E.: Contrasting effects of solar UV radiation on
686 dissolved organic sources for bacterial growth, Ecol. Lett., 4(5), 458–463, doi:10.1046/j.1461-
687 0248.2001.00245.x, 2001.

688 Weber, K. P. and Legge, R. L.: One-dimensional metric for tracking bacterial community
689 divergence using sole carbon source utilization patterns, J. Microbiol. Methods, 79(1), 55–61,
690 doi:10.1016/j.mimet.2009.07.020, 2009.

691 Weber, K. P. and Legge, R. L.: Community-Level Physiological Profiling, in Bioremediation,
692 pp. 263–281, Humana Press., 2010.

693 Williams, C. J., Yamashita, Y., Wilson, H. F., Jaffe, R. and Xenopoulos, M. A.: Unraveling the
694 role of land use and microbial activity in shaping dissolved organic matter characteristics in
695 stream ecosystems, Limnol. Oceanogr., 55(3), 1159–1171, doi:10.4319/lo.2010.55.3.1159,
696 2010.

697 Williams, C. J., Frost, P. C., Morales-Williams, A. M., Larson, J. H., Richardson, W. B.,

Chiandet, A. S. and Xenopoulos, M. A.: Human activities cause distinct dissolved organic matter composition across freshwater ecosystems, Glob. Chang. Biol., 22(2), 613–626, doi:10.1111/gcb.13094, 2016.

Wilson, H. F. and Xenopoulos, M. A.: Effects of agricultural land use on the composition of fluvial dissolved organic matter, Nat. Geosci., 2(1), 37–41, doi:10.1038/ngeo391, 2009.

Wu, Z., Wu, W., Lin, C., Zhou, S. and Xiong, J.: Deciphering the origins, composition and microbial fate of dissolved organic matter in agro-urban headwater streams, Sci. Total Environ., 659(163), 1484–1495, doi:10.1016/j.scitotenv.2018.12.237, 2019.

Xenopoulos, M. A., Barnes, R. T., Boodoo, K. S., Christina, C. D. A., Nu, D. B., Kothawala, D. N., Pisani, O., Solomon, C. T., Spencer, R. G. M., Williams, C. J. and Wilson, H. F.: How humans alter dissolved organic matter composition in freshwater : relevance for the Earth ' s biogeochemistry, , 3, doi:10.1007/s10533-021-00753-3, 2021.

Yamashita, Y., Scinto, L. J., Maie, N. and Jaffé, R.: Dissolved Organic Matter Characteristics Across a Subtropical Wetland's Landscape: Application of Optical Properties in the Assessment of Environmental Dynamics, Ecosystems, 13(7), 1006–1019, doi:10.1007/s10021-010-9370-1, 2010.

Table caption

Table 1 – Selected properties and dominant classification of sampling sites

Table 2 – Spectral properties (positions of maximum excitation (ex) and emission (em) peaks) of the eight PARARAC components identified in this study, general description and dominant sources based on previous studies.

Figure caption

Figure 1 – Map of the Lake Geneva Basin and the ten independent catchments sampled during this study.

Figure 2 – Boxplots of (A) Chl*a*, (B) SRP, (C) DIN, (D) DOC concentrations and (E) S_R values and (F) BR in agro-urban (grey) and forest-grassland (white) streams. The box represents the first and third quartile, the horizontal line corresponds to the median, the cross corresponds to the average, and the error bars correspond to the maximum and minimum. Mann Whitney unpaired *t*-test were used to test for statistical differences: ns represents not significant, ∗ =p<0.05, ∗∗ =p<0.01, ∗∗∗ =p<0.001, ∗∗∗∗ =p<0.0001.

Figure 3 – Boxplots of F_{Max} values of PARAFAC components in agro-urban (grey) and forest-grassland (white) streams. The box represents the first and third quartile, the horizontal line corresponds to the median, the cross corresponds to the average, and the error bars correspond to the maximum and minimum. Mann Whitney unpaired *t*-test were used to test for statistical differences: ns represents not significant, ∗ =p<0.05, ∗∗ =p<0.01, ∗∗∗ =p<0.001, ∗∗∗∗ =p<0.0001.

Figure 4 – PCA biplot, including loadings plot for the input variables and scores plot for stations. Markers are shaped according to the sampling period and colored according to a gradient of human disturbance (defined as the sum of % croplands and % urban areas, supplementary ordinal variable in the PCA).

Figure 5 – Boxplots of (A) BDOC concentrations, (B) constant decay *k*, (C) STRC and (D) LTRC pools in agro-urban (grey) and forest-grassland (white) streams. The box represents the first and third quartile, the horizontal line corresponds to the median, the cross corresponds to the average, and the error bars correspond to the maximum and minimum. Mann Whitney unpaired *t*-test were used to test for statistical differences: ns represents not significant, ∗ =p<0.05, ∗∗ =p<0.01, ∗∗∗ =p<0.001, ∗∗∗∗ =p<0.0001.

Figure 6 - Relationships between (A) BDOC, (B) decay constants and (C) the size of the STRC pools with the sum of initial F_{Max} values of C6, C7, and C8 components.

Figure 7 – Response ratio of PARAFAC components during incubation experiments with tf = day 28 and t0 = day 0. Grey bars represent threshold of significance above or below which significant production or consumption of component was identified. See text for details.

Figure 8 – Boxplots of (A) AA , (B) CAR, and (C) C&AA consumption in agro-urban (grey) and forest-grassland (white) streams. The box represents the first and third quartile, the horizontal line corresponds to the median, the cross corresponds to the average, and the error bars correspond to the maximum and minimum. Mann Whitney unpaired *t*-test were used to test for

statistical differences: ns represents not significant, * =p<0.05, ** =p<0.01, *** =p<0.001, **** =p<0.0001.

Figure 9 – Relationships between BR and (A) DOC concentrations, (B) the sum of initial F_{Max} values of C6, C7, and C8 components, and (C) initial F_{Max} values of C1 component

760 Table 1

761

Site	Area (km^2)	Mean elevation (masl)	Strahler order	Forest (%)	Croplands (%)	Urban areas (%)	Classification
1 - La Combe	39	1241	2	73	3	1	Forest-grassland
2 - Le Boiron	11	692	2	62	36	1	Forest-grassland
3 - Le Grand Curbit	14	614	2	24	70	4	Agro-urban
4 - La Venoge	228	696	4	31	60	6	Agro-urban
5 - La Mèbre	21	597	3	18	38	43	Agro-urban
6 - La Sorge	12	595	3	24	65	11	Agro-urban
7 - La Dranse	638		4	33	14	5	Forest-grassland
8 - Le Rhône	5238	2124	7	23	2	3	Forest-grassland
9 - La Veveyse	65	1105	5	45	20	6	Forest-grassland
10 - La Paudèze	16	775	4	33	40	25	Agro-urban

762

763 Table 2

764

Component	Max ex (nm)	Max em (nm)	Description & dominant sources
C1	<270	424	Widespread humic-like fluorophore, terrestrial[a,b] and/or photoproduced[c].
C2	<270 (330, 380)	498	Fulvic-like fluorophore, widepread, terrestrial origin[d,e].
C3	<270 (355)	438	Humic-like fluorophore, widespread, terrestrial origin[d].
C4	320	402	Low molecular weight humic-like fluorophore, related to agriculture[a,b,e].
C5	300	336	Protein-like fluorophore associated with biological production[f].
C6	<270	372	Anthropogenic humic-like fluorophore related to algal[g] or bacterial[f] production in urban areas[e,g].
C7	275	332	Tryptophan-like fluorophore, indicative of autochthonous production[b,c].
C8	270	304	Tyrosine-like fluorophore, indicative of autochthonous production[b,c].

[a] Stedmon & Markager, 2005; [b] Yamashita et al., 2010; [c] Massicote & Frenette 2011; [d] Graeber et al., 2012; [e] Lambert et al., 2017; [f] Stedmon et al., 2011; [g] Williams et al., 2016.

765

766 Figure 1

767

768

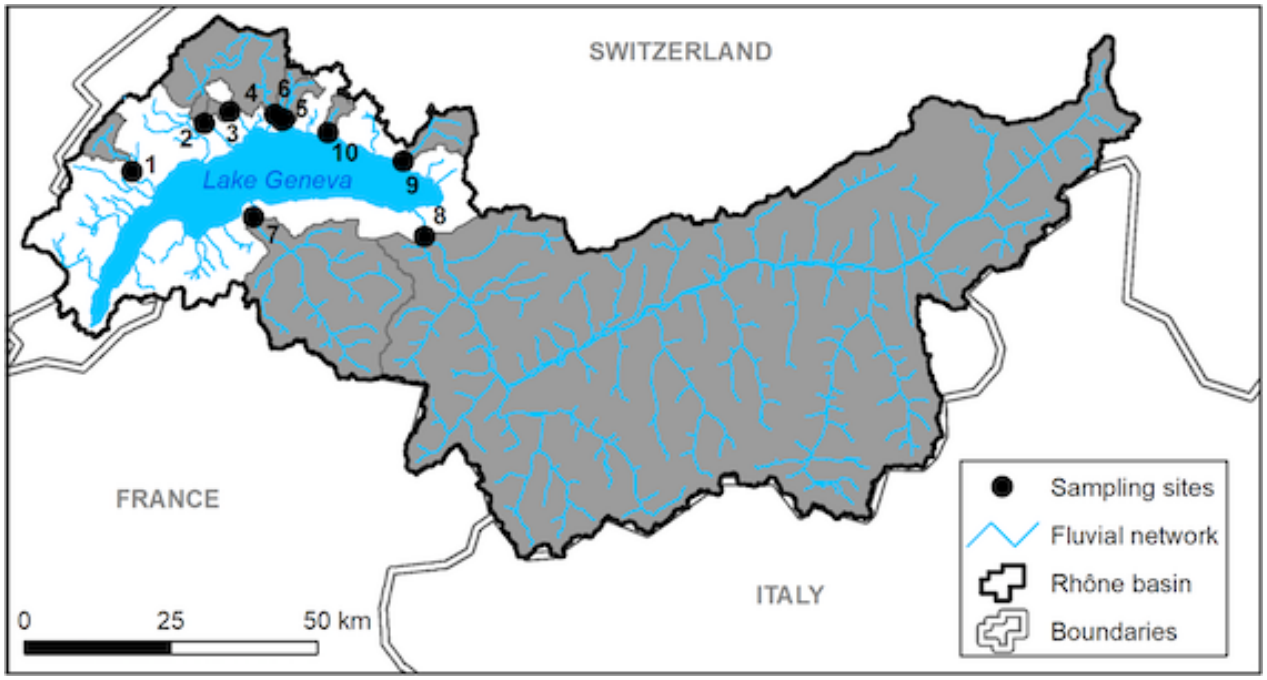

769

770 Figure 2

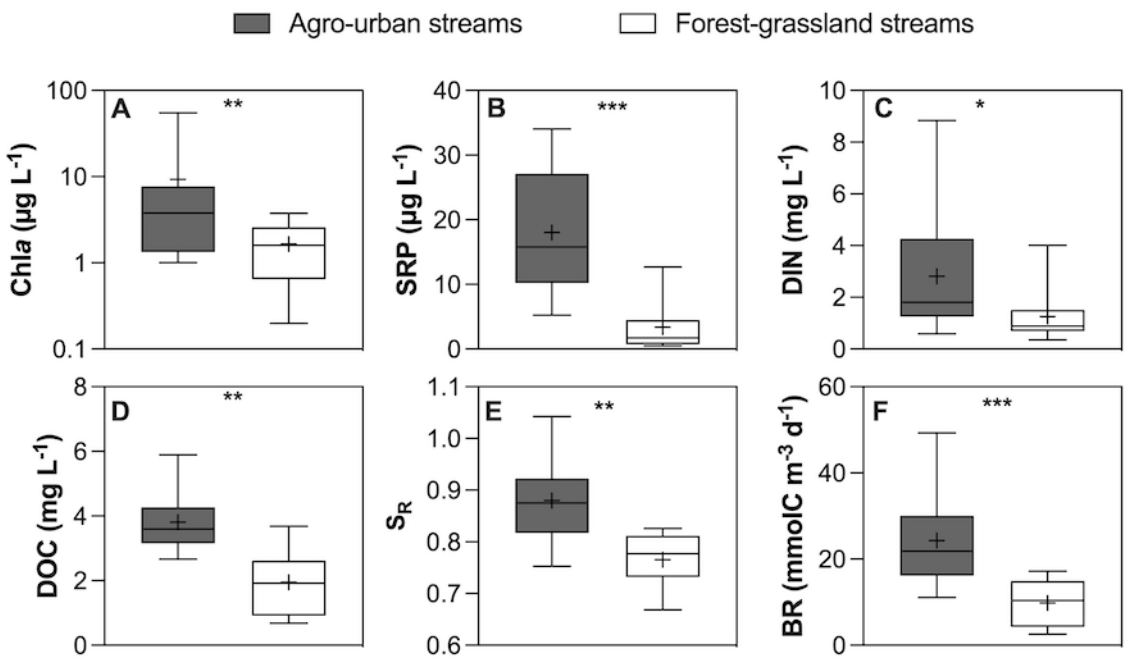

771

772 Figure 3

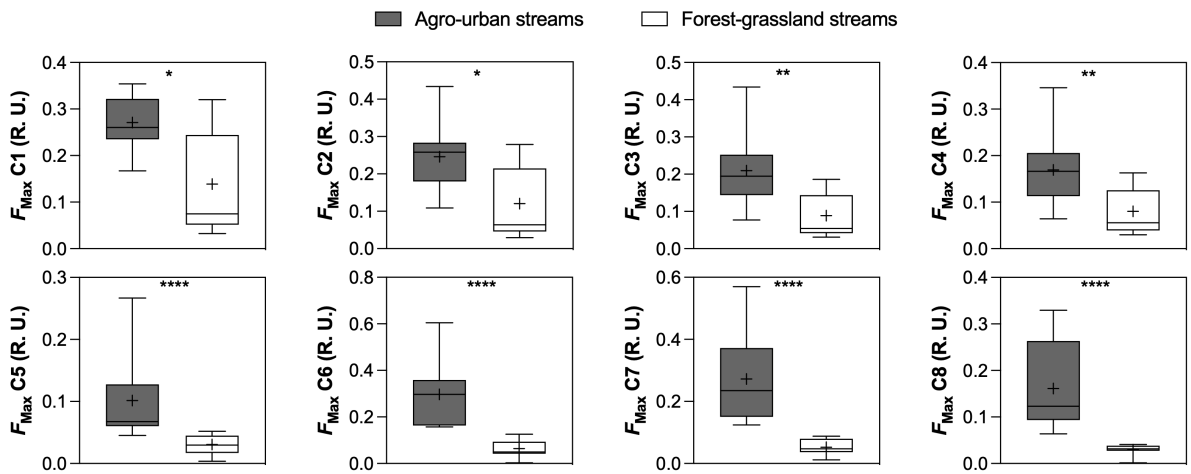

773

774 Figure 4

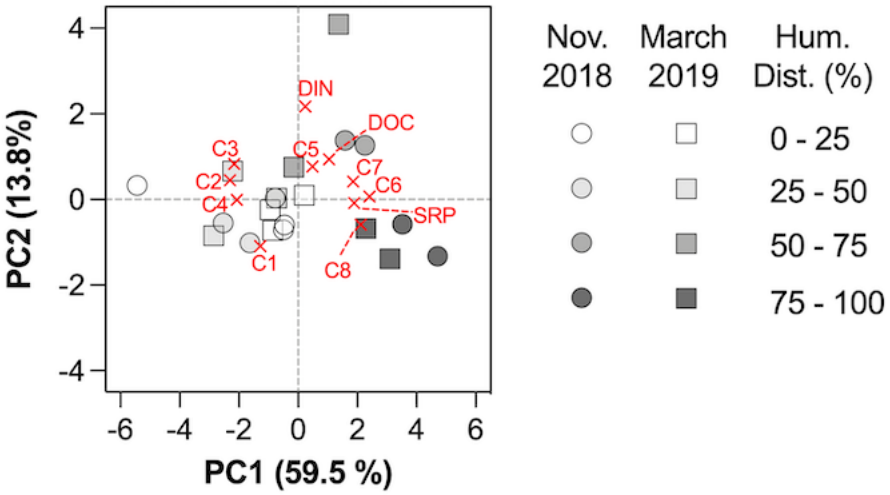

775

776 Figure 5

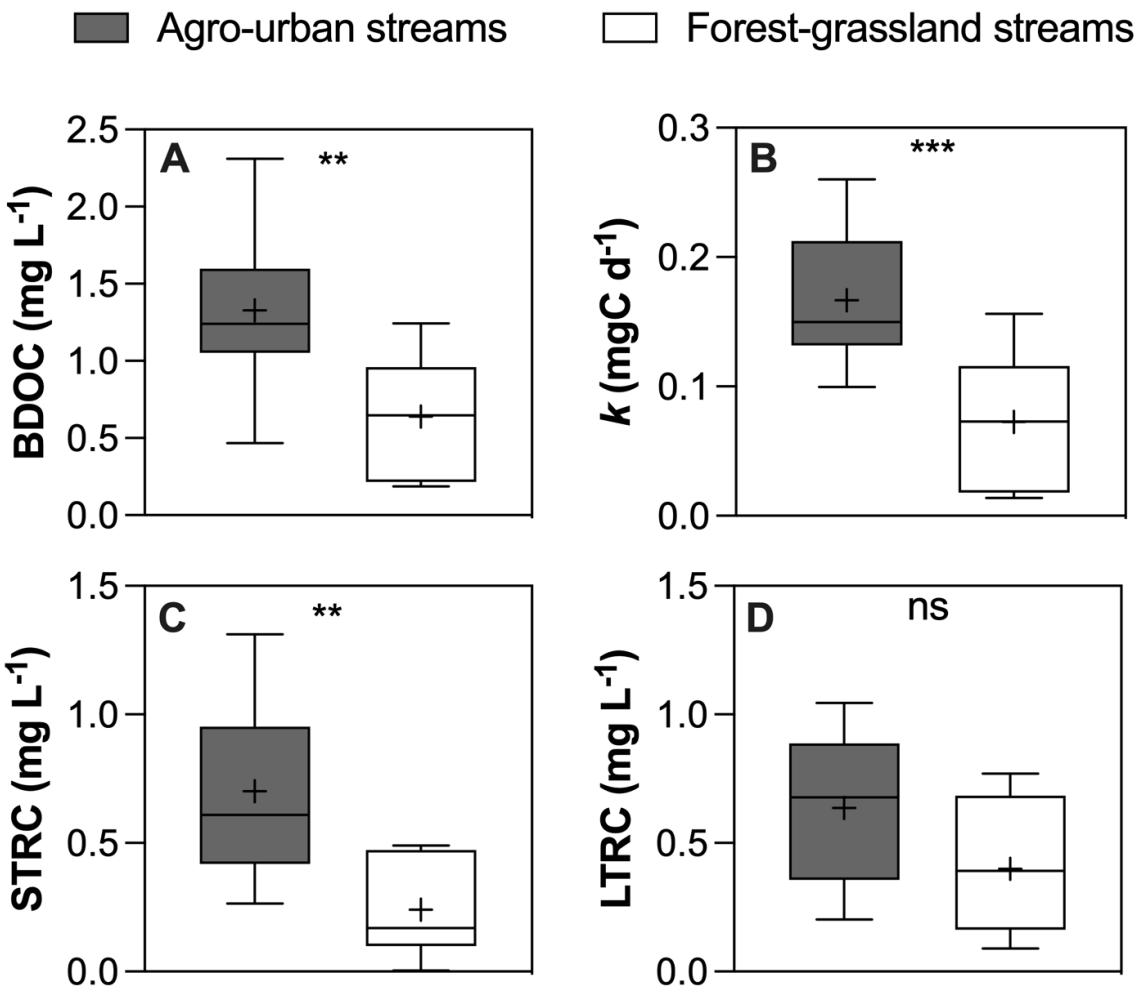

777

778 Figure 6

779

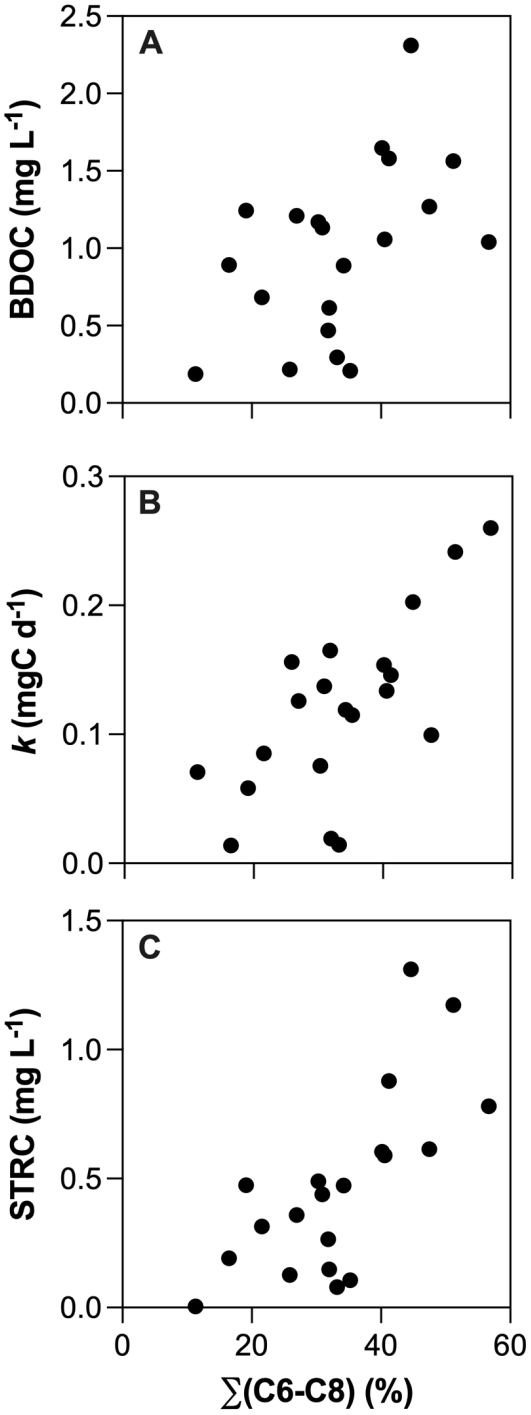

780

781 Figure 7

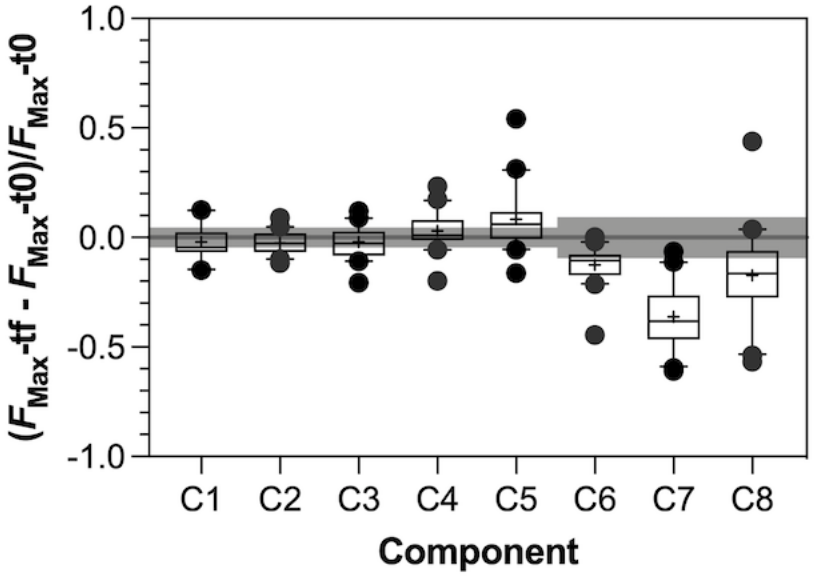

782

783 Figure 8

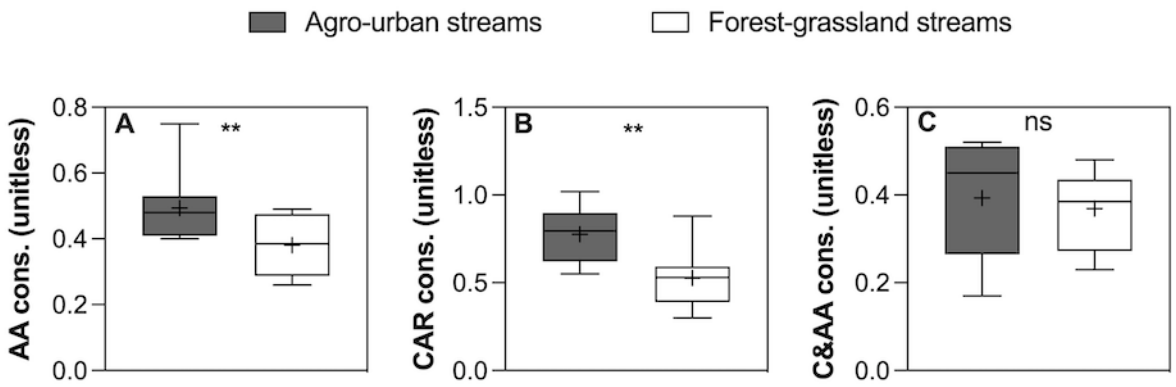

784

785 Figure 9

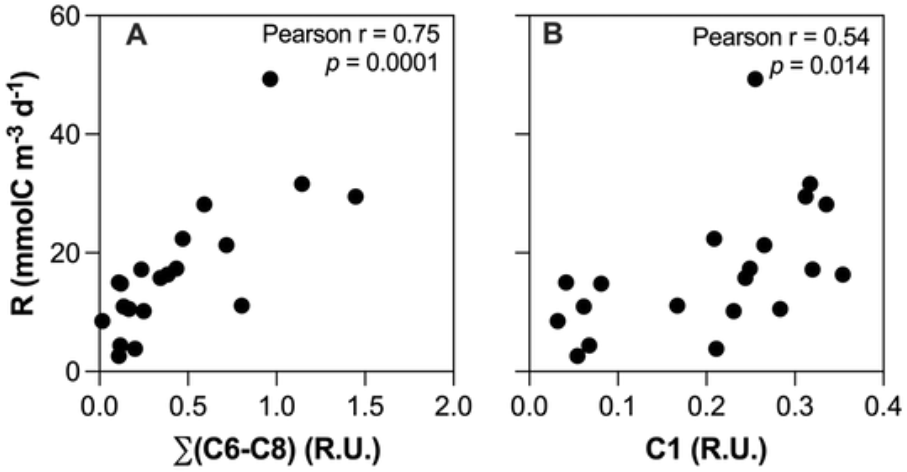

786